Geochemistry Geophysics Geosystems G3

Research Letter
Volume 12, Number 9
16 September 2011
Q09007, doi:10.1029/2011GC003691
ISSN: 1525-2027

Published by AGU and the Geochemical Society

Changes in micronutrient supply to the surface Southern Ocean (Atlantic sector) across the glacial termination

Katharine R. Hendry
Department of Marine Chemistry and Geochemistry, Woods Hole Oceanographic Institution, Woods Hole, Massachusetts 02543, USA (khendry@whoi.edu)

School of Earth and Ocean Sciences, Cardiff University, Main Building, Park Place, Cardiff CF10 3AT, UK

Rosalind E. M. Rickaby
Department of Earth Sciences, University of Oxford, South Parks Road, Oxford OX1 3AN, UK

Claire S. Allen
British Antarctic Survey, Madingley Road, Cambridge CB3 0ET, UK

[1] Major deepwater masses upwell and reach the surface in the Southern Ocean, forming an important conduit supplying nutrients and micronutrients to the surface and playing a key role in the regulation of global climate through ocean-atmosphere gas exchange. Here, we reconstruct changes in micronutrient distribution in this region in response to past changes in upwelling, oceanic mixing, and sea-ice seasonality. We present two downcore $(Zn/Si)_{opal}$ records from the Scotia Sea and Drake Passage region, which we interpret in the context of micronutrient distribution in the Atlantic sector of the Southern Ocean over the last glacial termination. Previous work shows that micronutrient availability in the surface waters in the South Atlantic appear to be controlled dominantly by upwelling and mixing of micronutrient rich deepwaters, which are additionally fuelled by the terrestrial sediment sources of the Scotia Arc and South Georgia. This is supported by our reconstructions, which show micronutrient availability to the west of the Scotia Arc and South Georgia are consistently lower than to the east over the last glacial termination due to downstream transport and mixing into surface waters of continentally derived material in the Antarctic Circumpolar Current. Micronutrient availability in this region was at a minimum from 20 to 25 ky BP, coinciding with maximum sea-ice coverage, and increased due to an expansion of the seasonal sea-ice zone and increased mixing of subsurface waters. Our findings are consistent with largely diminished upwelling of micronutrients during the maximum glacial extent, and reduced mixing due to the presence of persistent sea-ice. During the deglacial there was an increase in micronutrient availability, as well as other nutrients and inorganic carbon, within the Antarctic Circumpolar Current as a result of an increase in deep oceanic upwelling, mixing and strengthened zonal transport.

Components: 6800 words, 5 figures, 1 table.

Keywords: deglaciation; diatom opal; westerlies; zinc.

Index Terms: 0470 Biogeosciences: Nutrients and nutrient cycling (4845, 4850); 0473 Biogeosciences: Paleoclimatology and paleoceanography (3344, 4900); 4912 Paleoceanography: Biogeochemical cycles, processes, and modeling (0412, 0414, 0793, 1615, 4805).

Received 9 May 2011; **Revised** 4 August 2011; **Accepted** 4 August 2011; **Published** 16 September 2011.

Hendry, K. R., R. E. M. Rickaby, and C. S. Allen (2011), Changes in micronutrient supply to the surface Southern Ocean (Atlantic sector) across the glacial termination, *Geochem. Geophys. Geosyst.*, *12*, Q09007, doi:10.1029/2011GC003691.

1. Introduction

1.1. Micronutrients in the Southern Ocean

[2] The Southern Ocean is a major High Nutrient Low Chlorophyll region (HNLC [*Minas and Minas*, 1992]), characterized by low utilization of major nutrients, such as nitrate, phosphate and silicic acid. The supply of micronutrients (e.g., iron, zinc, cadmium etc.), in addition to light and grazing pressures, is thought to limit productivity in HNLC regions [e.g., *Brzezinski et al.*, 2005]. Previous studies have focused on understanding past changes in the supply of micronutrients to determine the degree to which subpolar biology is nutrient-limited in the southern hemisphere over glacial-interglacial timescales [e.g., *Martin*, 1990; *Ellwood and Hunter*, 2000b; *Röthlisberger et al.*, 2004; *Edwards et al.*, 2006; *Beucher et al.*, 2007]. In addition, understanding the past distribution of micronutrients that are largely derived from oceanic sources [*Meskhidze et al.*, 2007] is important for reconstructing past changes in upwelling and mixing. Such processes play crucial roles in the supply of preformed nutrients to global oceans, air-sea gas exchange and carbon cycling [e.g., *Marinov et al.*, 2008].

[3] Today, the micronutrients that reach the surface waters of the Atlantic sector of the Southern Ocean are largely supplied through oceanic sources (upwelling and lateral advection), and are inherently linked to prevailing wind direction and strength [*Meskhidze et al.*, 2007]. The eastward-flowing Antarctic Circumpolar Current (ACC) is confined bathymetrically in the Drake Passage and Scotia Sea, in the region of the Polar Front (Figure 1) [*Naveira Garabato et al.*, 2002]. Upwelling of deep water by Ekman pumping in the Southern Ocean is driven by the action of the prevailing strong westerly winds on the ACC. The strength of the pumping is influenced by both the strength of these "westerlies" and their position in relation to the ACC: stronger, and more southerly winds (aligned with the ACC) result in stronger Ekman pumping [*Toggweiler and Samuels*, 1993; *Toggweiler et al.*, 2006]. Vertical upwelling processes, tied to bathymetric features, oceanic fronts and eddy generation, are important for micronutrient supply from subsurface, nutrient-rich water in the Scotia Sea [*Holm-Hansen et al.*, 2005; *Kahru et al.*, 2007], and other open ocean regions of the Southern Ocean [*Measures and Vink*, 2001]. In addition to these field studies, modeling studies suggest that upwelling of deepwater contributes approximately 99% of micronutrients to the Southern Ocean, far outweighing input from atmospheric sources [*Lefèvre and Watson*, 1999].

[4] Several field studies highlight the importance of terrigenous sediments in sourcing trace metals to the oceans, and interaction with near surface ocean currents and sea-ice formation for the transportation of such micronutrients to surface waters of the Southern Ocean (e.g., Drake Passage [*Dulaiova et al.*, 2009]; Crozet Islands [*Planquette et al.*, 2007]; West Antarctic Peninsula [*Ardelan et al.*, 2010, *Hendry et al.*, 2010]). Such naturally micronutrient-fertilized regions are characterized by high primary productivity [e.g., *Clarke et al.*, 2008; *Hernandez-Sanchez et al.*, 2010]. The importance of the prevailing winds and ocean currents in the Southern Ocean manifests in an inherent east-west asymmetry in the Atlantic sector, with high productivity downstream of the terrestrial sediment sources of the Scotia Arc and South Georgia (Figure 1) [e.g., *Korb et al.*, 2004]. This asymmetry is exaggerated by the flow of Lower Circumpolar Deep Water, which mixes in with nutrient-rich deep Pacific waters in the Drake Passage, and only encroaches the surface to the south of the ACC and when the ACC leaves the Scotia Basin [*Naveira Garabato et al.*, 2003].

[5] Here we use diatom-based paleoproxies, combining fossil assemblage data and geochemistry, from sediment cores recovered from the Scotia Sea to reconstruct changes in the surface availability of micronutrients since the last glacial. We use the $(Zn/Si)_{opal}$ of diatoms as a measure of micronutrient availability, which, in this region of the South Atlantic, can be used as a proxy for the strength of lateral transport, upwelling or deep-ocean mixing. Our results, together with published records from the Atlantic sector of the Southern Ocean, are consistent with changes in micronutrient supply via enhanced oceanic upwelling and mixing, linked to an expansion of the seasonal sea-ice zone.

1.2. Diatom Paleoproxies: Species Counts and Geochemistry

[6] As a result of variation in habitat preference during life, diatom fossil assemblages can reflect past changes in surface hydrography despite influence from postmortem effects such as grazing, remobilization and dissolution [*Crosta et al.*, 1998]. For example, the pennate diatom species *Fragilariopsis curta* and *F. cylindrus* occur in core top sediments underlying regions that experience sea-ice cover for at least part of the year [e.g.,

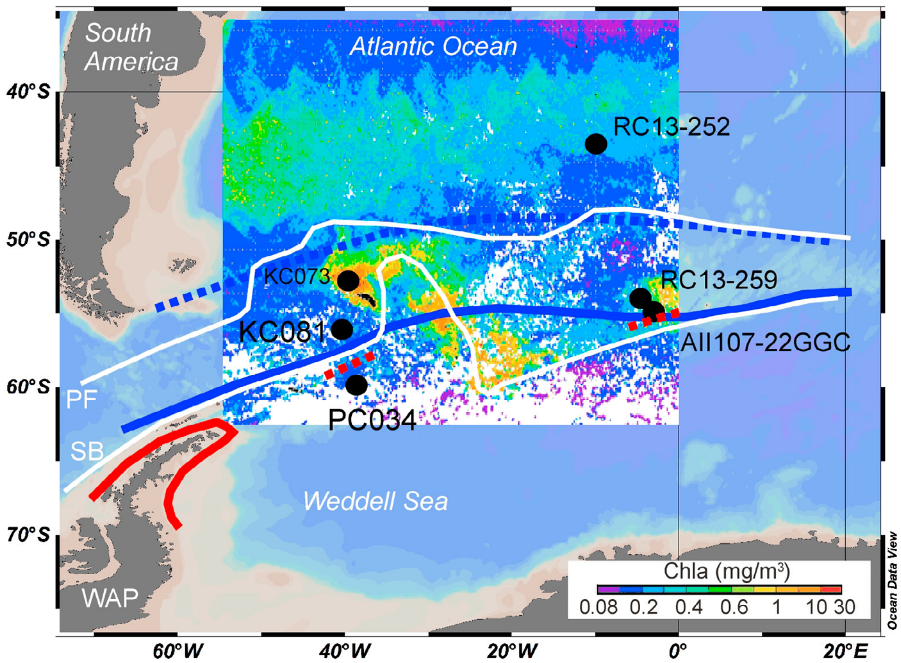

Figure 1. Map showing location of cores KC081 and PC034 (this study), KC073 [*Allen et al.*, 2005] and AII107–22GGC, RC13–252 and RC13–259 [*Ellwood and Hunter*, 2000b]. The colored contours show chlorophyll a (Chl*a*) from ocean color satellite data (http://disc.sci.gsfc.nasa.gov/), with higher Chl*a* levels downstream of the eastward-flowing ACC during a late seasonal bloom (April 2000). Also shown are the estimated positions of the modern Polar Front (PF) and the Southern Boundary of the Antarctic Circumpolar Current (SB [*Moore et al.*, 1999; *Meredith et al.*, 2008]). The blue lines show the position of the winter sea-ice extent; the red lines show the position of the summer sea-ice extent (solid line for the modern, dashed line for the Last Glacial Maximum [*Abelmann et al.*, 2006; *Allen et al.*, 2011]).

Armand et al., 2005]. Consequently, for regions far from the continental glacial meltwaters, the presence of *F. curta* + *F. cylindrus* in downcore records at abundances >3% is used to indicate the presence of winter sea ice [*Gersonde and Zielinski*, 2000].

[7] The zinc content of diatom frustrules (normalized to silicon, $(Zn/Si)_{opal}$), with careful cleaning and preparation, can be used as a paleoproxy for past micronutrient concentrations [e.g., *Ellwood and Hunter*, 1999, 2000a, 2000b; *Hendry and Rickaby*, 2008; *Andersen et al.*, 2011]. Laboratory cultures of both marine and freshwater diatoms show a relationship between $(Zn/Si)_{opal}$ and biologically available free Zn^{2+} ions [*Ellwood and Hunter*, 2000a; *Jaccard et al.*, 2009]. Dissolution experiments show that the Zn/Si released through time is constant for a given opal sample, indicating that the Zn content of diatom frustrules is homogeneous [*Ellwood and Hunter*, 2000a; *Hendry and Rickaby*, 2008]. Field tests support the laboratory findings, and show that $(Zn/Si)_{opal}$ and the Zn isotopic composition of diatom opal also relates to trace metal availability, which is often coupled with biological productivity and nutrient uptake in regions such as the Southern Ocean [*Jaccard et al.*, 2009; *Hendry and Rickaby*, 2008; *Andersen et al.*, 2011]. Sediment trap and core top studies show $(Zn/Si)_{opal}$ signatures are transferred faithfully to sediments [*Hendry and Rickaby*, 2008], such that $(Zn/Si)_{opal}$ is a useful paleoproxy, especially in the Southern Ocean where carbonate-based proxies are poorly preserved.

[8] Here, we use a combination of diatom species counts and opal geochemistry to address changes in micronutrient availability and sea-ice seasonality over the last glacial termination and how it relates to changes in winds, oceanic upwelling, and sea-ice seasonality during the deglaciation.

2. Methods and Materials

[9] To investigate past hydrographic and nutrient changes in surface waters, diatoms were separated from two sediment cores from the Scotia Sea and Drake Passage, KC081 and PC034 obtained from the British Antarctic Survey (Figure 1). Radiocarbon dating of sediments from the Southern Ocean

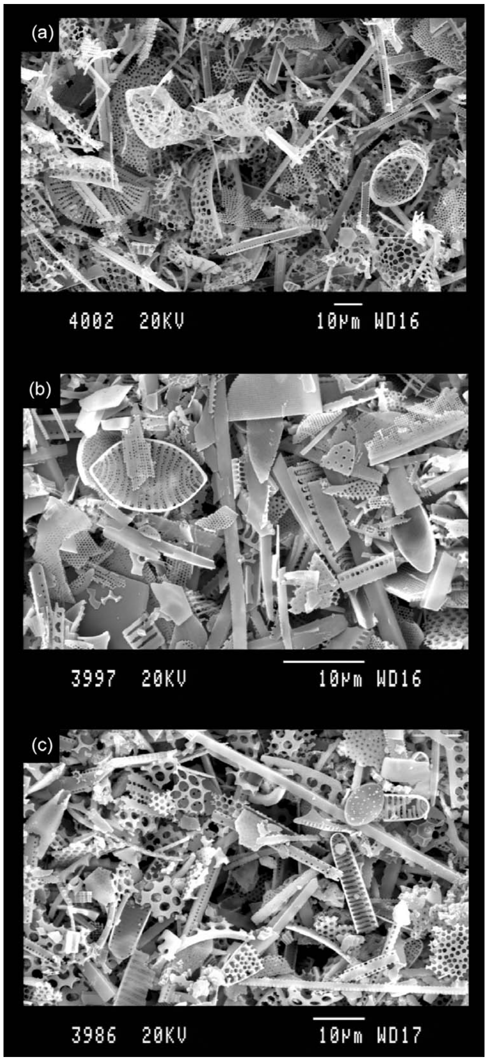

Figure 2. SEM images of cleaned opal from (a) KC081 (135 cm depth), (b) PC034 core top and (c) PC034 220cm depth, after heavy liquid separation.

is often hampered by the lack of carbonate and poorly constrained reservoir ages, but can be achieved through a combination of magnetostratigraphy and biostratigraphy. The Last Glacial Maximum (LGM) can be constrained by a peak in abundance of the diatom *Eucampia antarctica* [*Burckle and Cooke*, 1983] and the radiolarian *Cycladophora davisiana* [*Hays et al.*, 1976]. Peak abundances in *E. antarctica* and *C. davisiana* have been observed to be asynchronous in the Scotia Sea, with the peak in *E. antarctica* typically preceding the *C. davisiana* peak by 1000 years, most likely as a result of the two species inhabiting different water depths and environments [*Burckle and Cooke*, 1983; *Gersonde et al.*, 2003]. The age model for KC081 is based on radiocarbon dates (auxiliary material), and the LGM is additionally constrained by the first downcore peak in magnetic susceptibility and *E. antarctica* abundance [*Burckle and Cooke*, 1983; *Allen et al.*, 2011].[1] Core PC034 has not been radiocarbon dated, due to the lack of preserved carbonate, but the LGM is constrained by the first downcore peak in magnetic susceptibility and *C. davisiana* abundance [*Hays et al.*, 1976; *Allen et al.*, 2011]. Additionally, the glacial has been dated in PC034 by tying the magnetic susceptibility to EPICA dust records [*Pugh et al.*, 2009; *Allen et al.*, 2011].

[10] For the opal trace metal analyses, sediment samples were cleaned for organic matter and carbonates, disaggregated, and separated from lithogenic particles using heavy liquid flotation (LST FastFloat) repeatedly until only clean, cream-colored opal remained [*Hendry and Rickaby*, 2008]. SEM images show the samples to comprise pure diatoms at this stage (Figure 2). The samples were then chemically cleaned using a series of oxidative and reductive reagents [*Shemesh et al.*, 1988; *Ellwood and Hunter*, 1999; *Hendry and Rickaby*, 2008] (auxiliary material). While some studies have shown rigorous cleaning is not essential [*Lal et al.*, 2006] other studies show, using the isotopic signature of diatoms and sequential leaching, that the steps are essential to reach a clean "plateau" representing the true $(Zn/Si)_{opal}$ signal [*Ellwood and Hunter*, 1999; *Hendry and Rickaby*, 2008; *Andersen et al.*, 2011].

[11] The diatom opal was dissolved at room temperature in dilute hydrofluoric acid, which results in quantitative recovery of the biogenic silicon. A small aliquot was taken to measure silicon concentrations and the remainder was used to measure $(Al/Si)_{opal}$ and $(Zn/Si)_{opal}$ using a matrix-matched standard-sample bracketing method by Quadrupole Inductively Coupled Plasma Mass Spectrometry (Perkin Elmer Elan 6100DRC Q-ICP-MS; University of Oxford; see *Hendry and Rickaby* [2008] for details). Results where the relative standard deviation (RSD) was greater than 15%, as a result of machine instability, were rejected.

3. Results and Discussion

3.1. Sea-Ice Diatoms and Sea-Ice Seasonality

[12] PC034 and KC081 were selected for study according to their geographical location with respect

[1] Auxiliary materials are available in the HTML. doi:10.1029/2011GC003691.

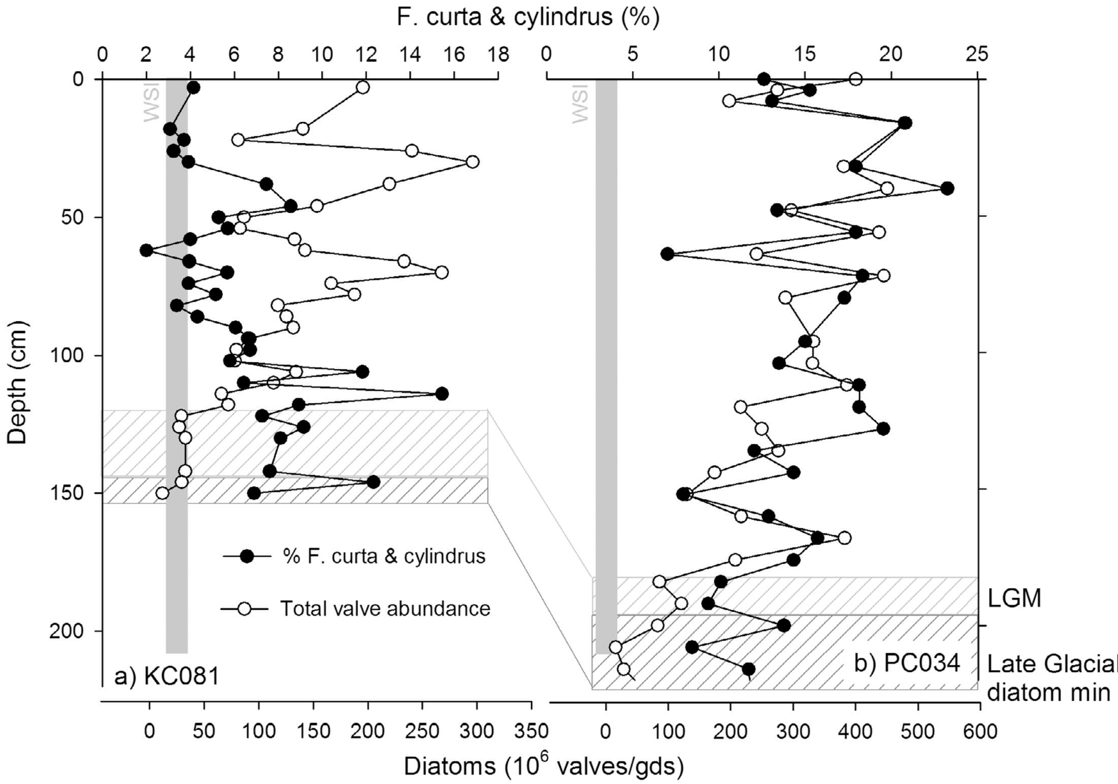

Figure 3. Diatom records from (a) KC081 and (b) PC034, showing total diatom counts (10^6 valves/g dry sediment; open symbols) and % *F. curta and F. cylindrus* (solid symbols). Data from *Allen et al.* [2011]. The hatched regions show approximate depths for the Last Glacial Maximum (LGM) and the late glacial diatom minimum. The solid gray bar shows 3–4% sea-ice diatoms, an indicator of Winter Sea-Ice (WSI).

to the ACC, and average Winter Sea-Ice (WSI) extent. Today the average WSI extends further north than site PC034, and is just to the south of site KC081 (Figure 1). This is reflected in the core top diatom assemblage in PC034, as *F. curta* + *F. cylindrus* constitute >3% of the diatom counts (Figure 3). The presence of >3% *F. curta* + *F. cylindrus* at KC081 is either a result of the occasional presence of WSI, or loss of recent surface material yielding a sea-ice limit associated with the Late Holocene neoglacial period [*Allen et al.*, 2011].

[13] During the last glacial, sites in the far north Scotia Sea and Falkland Trough (e.g., KC073, 52° 09.2′S, 41° 10.7′W) contain more than 3% of the sea ice diatoms *F. curta* + *F. cylindrus* indicating the presence of WSI [*Allen et al.*, 2005]. For site KC073, the percentage *F. curta* + *F. cylindrus* falls rapidly after approximately 20 ky BP, signifying permanently open ocean conditions throughout the year. In contrast, the Scotia Sea cores KC081 and PC034 to the south indicate that WSI retreated later in the deglacial. For KC081, the percentage *F. curta* + *F. cylindrus* falls to modern values (~3–4%) by approximately 10 ky BP; in PC034, *F. curta* + *F. cylindrus* occur at abundances much greater than 3% throughout the Holocene confirming that the WSI extends north of/expands over the site in most years (Figure 3).

[14] Both sites today are north of the Summer Sea Ice (SSI) extent. The presence of *F. curta* + *F. cylindrus* throughout the two records confirms that both sites have been the seasonal sea-ice zone over the last glacial termination. However, total diatom valve counts are low during the late glacial (pre-22 ky BP) in both cores, suggesting reduced export production (combined with sediment dilution effects [*Allen et al.*, 2011]). Such reduced export production could have resulted from more persistent sea-ice, especially for site PC034, which was near the SSI edge and may have even had intermittent SSI cover before ~22 ky BP [*Gersonde et al.*, 2005; *Allen et al.*, 2011]. Both cores show an increase in total diatom concentration from 20 to 22 ky BP and into the deglacial, earlier than the decline in sea-ice diatoms observed in KC081, and

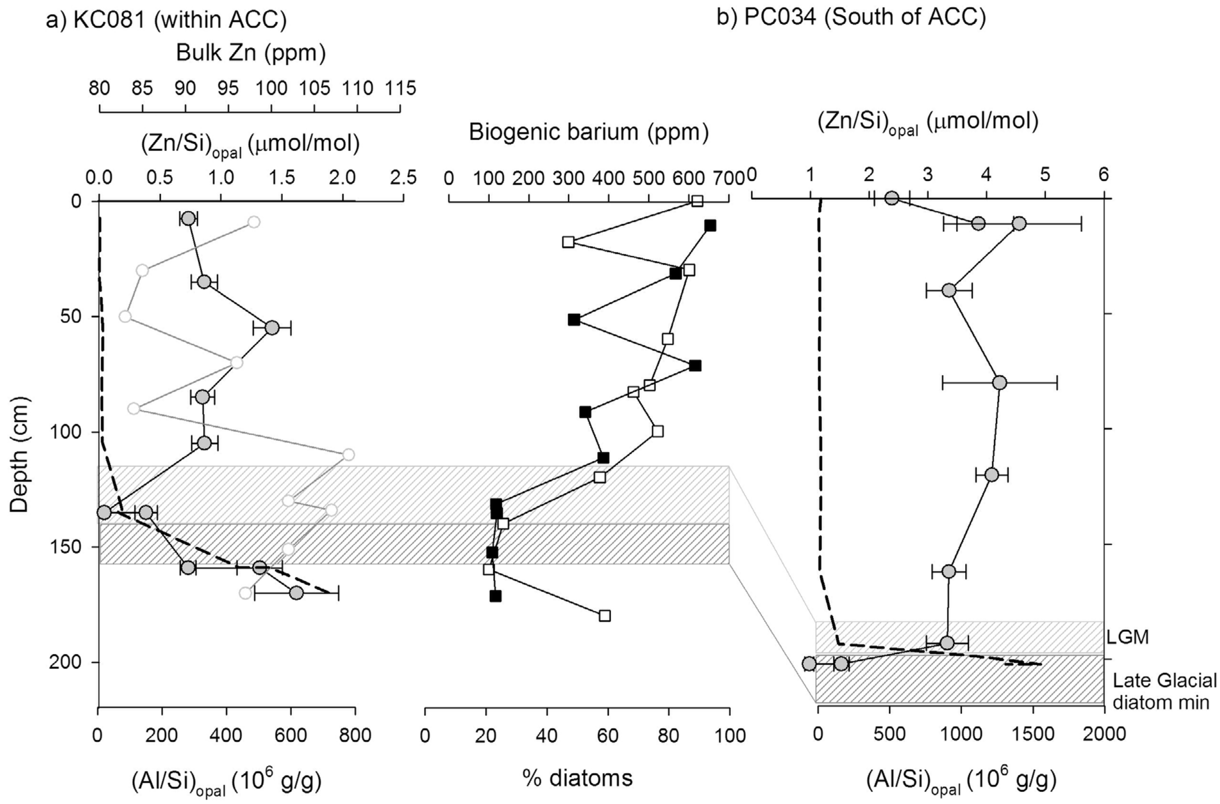

Figure 4. $(Zn/Si)_{opal}$ results for (a) KC081 and (b) PC034 (solid gray circles, error bars show $\pm 2\sigma_{SD}$). The $(Al/Si)_{opal}$ results are shown by the thick dashed line. Also shown for KC081 are bulk Zn (open gray circles), the percentage of the sediment comprising diatoms (open squares) and biogenic barium (closed squares). The hatched regions show approximate depths for the Last Glacial Maximum (LGM) and the late glacial diatom minimum.

restoration of open water conditions for a greater part of the year (Figure 3). KC081 biogenic barium, which has been corrected for lithogenic barium and can be used as a proxy for productivity [*Dymond et al.*, 1992], also shows a permanent increase during the early deglacial and is closely related to the total percentage of diatoms in the sediments (Figure 4a). This relatively early increase in diatom production and the persistence of *F. curta* + *F. cylindrus* at both sites suggests a decoupling between SSI and WSI [*Allen et al.*, 2011], resulting in a large areal extent of the seasonal sea-ice zone during the LGM and deglacial.

3.2. $(Zn/Si)_{opal}$ Records and Zonal Micronutrient Distribution

[15] Downcore $(Zn/Si)_{opal}$ values for KC081 range from 0.04 to 1.5 μmol/mol and in PC034 range from 1 to 5 μmol/mol (Figure 4). There is a minimum in the $(Zn/Si)_{opal}$ values during the late glacial (~22 ky BP) for both cores followed by an increase starting at the end of the glacial and into the deglaciation, coinciding with an increase in diatom valve abundance (Figure 3). The increase in both valve abundance and $(Zn/Si)_{opal}$ is more pronounced in the southern site, PC034.

[16] We can use the Al content of the diatom opal to demonstrate that the $(Zn/Si)_{opal}$ results are not affected by diagenesis. Holocene $(Al/Si)_{opal}$ ranges from 1.2 to 2.1 × 10^{-5} g/g for KC081, increasing to 0.0008 g/g at the glacial maximum; similarly, PC034 $(Al/Si)_{opal}$ ranges from 0.1 to 2.7 × 10^{-5} g/g, increasing to 0.0016 g/g at the glacial maximum (Table 1 and Figure 4). The $(Al/Si)_{opal}$ values correspond well with bulk Al and magnetic susceptibility [*Allen et al.*, 2011], and are most likely recording a secondary signal of sedimentary processes.

[17] Al is rapidly incorporated into biogenic opal at the sediment-water interface during early diagenesis, stabilizing the opal against further dissolution and chemical change [*Van Bennekom*, 1981; *Van Bennekom et al.*, 1989; *Dixit and Van Cappellen*, 2002; *Koning et al.*, 2007; *Hendry and Rickaby*, 2008; *Hendry et al.*, 2010]. If Zn was also adsorbed during such diagenesis processes one would expect to observe a relationship between $(Zn/Si)_{opal}$ and

Table 1. $(Al/Si)_{opal}$ and $(Zn/Si)_{opal}$ Results for Cores KC081 and PC034[a]

Core	Depth (cm)	$(Al/Si)_{opal}$ (μg/g)	$(Zn/Si)_{opal}$ (μmol/mol)
KC081	0	8.2 (0.3)	0.73 (0.04)
	35	7.2 (0.3)	0.86 (0.05)
	35	17.4 (0.8)	1.42 (0.08)
	85	14.6 (0.5)	0.85 (0.05)
	105	16.7 (0.5)	0.86 (0.05)
	135	79.6 (2.6)	0.04 (0.01)
	135	63.3 (1.6)	0.38 (0.05)
	159	442 (12)	0.73 (0.03)
	159	535 (26)	1.32 (0.09)
	170	718 (63)	1.62 (0.17)
PC034	0	18.6 (0.9)	2.39 (0.15)
	11	3.6 (0.1)	3.86 (0.29)
	40	15.3 (0.7)	3.36 (0.19)
	80	9.3 (0.7)	4.22 (0.49)
	120	22.1 (0.5)	4.09 (0.14)
	162	11.9 (0.3)	3.36 (0.15)
	193	143 (6)	3.33 (0.18)
	202	1550 (25)	1.53 (0.06)
	202	1300 (24)	0.98 (0.04)

[a]Numbers in parentheses are $1\sigma_{SD}$.

$(Al/Si)_{opal}$. It is clear that there is no relationship between $(Al/Si)_{opal}$ and $(Zn/Si)_{opal}$ ratios from the same samples (Table 1 and Figure 4), which indicates $(Zn/Si)_{opal}$ is recording a primary surface signal rather than a secondary sedimentary signal. Furthermore, there is no correlation between bulk Zn in the sediments and $(Zn/Si)_{opal}$ suggesting no impact from clay contaminants or surface coatings (Figure 4a).

[18] Our $(Zn/Si)_{opal}$ values are in the same range as previous records published by *Ellwood and Hunter* [2000a, 2000b] and agree well with other Southern Ocean core top records [*Hendry and Rickaby*, 2008; *Andersen et al.*, 2011]. However, in comparison to the other sites, from this study and *Ellwood and Hunter* [2000b], the $(Zn/Si)_{opal}$ values at KC081 are consistently low (Figure 4). We may account for this observation due to the maintenance of a zonal east-west asymmetry in the Drake Passage region, with higher nutrients to the east of South Georgia, within the ACC since the glacial. The persistent westerlies transport micronutrients from the continental shelf around South Georgia and the West Antarctic Peninsula by ocean currents in an eastward direction [*Korb et al.*, 2004] (Figure 1).

3.3. The Impact of Changes in Upwelling and Mixing on Micronutrient Supply Over the Last Glacial Termination

[19] Our $(Zn/Si)_{opal}$ results, and previously published records, do not resemble the temporal variations in dust supply to the Southern Ocean as recorded in ice cores from Antarctica [e.g., *Delmonte et al.*, 2002]. This further suggests that the $(Zn/Si)_{opal}$ records reflect supply of Zn from vertical upwelling of deepwater, and lateral transport and mixing of dissolved shelf sediments, rather than from direct atmospheric sources. Here, we show these results are consistent, within the limits of inherent uncertainties, with a geographically widespread increase in Zn availability south of the Polar Front from the late glacial into the deglacial. We suggest that an expansion of the seasonal sea-ice zone, and intense oceanic upwelling driven by the poleward migration of strong westerlies led to this increase in micronutrient availability.

[20] One important caveat with this study is the lack of constraint on whether $(Zn/Si)_{opal}$ is recording upwelling of deepwaters, or subsurface mixing of waters and sediment derived trace metals, both of which are likely to be important for the supply of dissolved Zn to surface waters. Furthermore it is often difficult to say whether the proxy is recording simply the supply of trace metals, or if there is also a productivity and utilization signal [*Hendry and Rickaby*, 2008], especially in HNLC regions such as the Southern Ocean trace metal supply and biological productivity are inherently linked.

[21] Precise timing and correlation of the $(Zn/Si)_{opal}$ records are not possible due to the limitations of the age models in carbonate-poor regions of the Southern Ocean. However, we have attempted to portray the general trends by calculating mean $(Zn/Si)_{opal}$ values for 5000 year age bins for the Antarctic and subantarctic regions respectively (Figure 5; for all data see auxiliary material).

3.3.1. Antarctic Zone

[22] The mean values for the cores "downstream" of terrigenous sources and in regions experiencing upwelling of LCDW (AII-107-22GC and RC13–259, and PC034 to the south of the ACC and near the West Antarctic Peninsula islands) show significantly higher $(Zn/Si)_{opal}$ than the "upstream" site (as discussed above) during all the time periods considered. During the glacial (>20 ky BP) the "downstream" sites, and the site to the north of the ACC (RC13–252) show very similar micronutrient availability. The individual downcore records (Figures 3 and 4) exhibit minima in both percentage diatom valves and $(Zn/Si)_{opal}$ before 20 ky BP and subsequently increase at the late glacial and early deglacial.

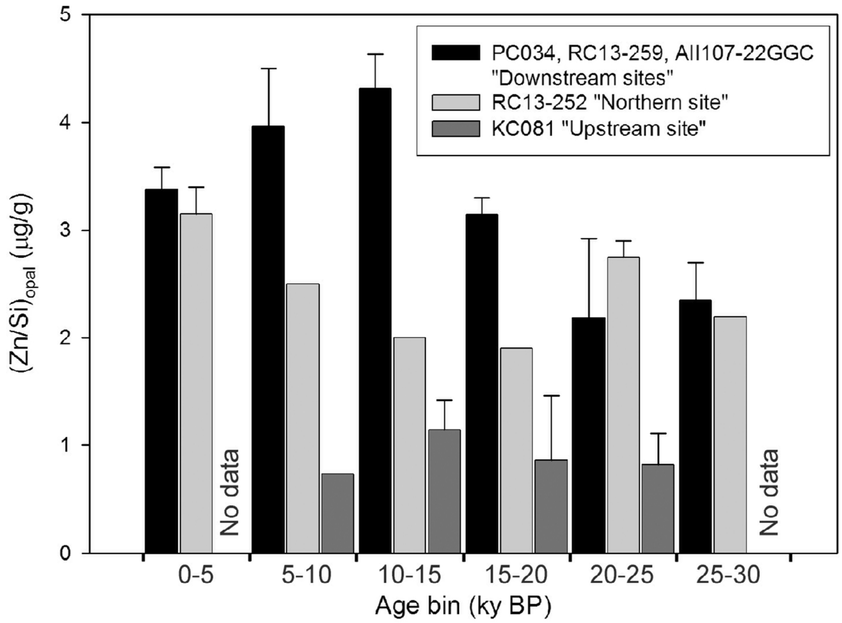

Figure 5. Changes in $(Zn/Si)_{opal}$ since the late glacial. The bars show the mean values of diatom $(Zn/Si)_{opal}$ for 5 ky age bins (e.g., 0–5 ky includes from 0 to <5 ky). The black bars show mean data for all sites "downstream" of terrigenous sources of micronutrients and LCDW upwelling (PC034, AII-107-22GC, RC13–259); the pale gray bars show site RC13–252 to the north of the ACC; the dark gray bars show site KC081 "upstream" of terrigenous sources of micronutrients and where LCDW is at depth. After the late glacial (~22 ky BP) Antarctic temperatures increased, leading to a retreat in summer sea-ice and an expansion of the seasonal sea-ice zone. This opened up a greater area (for at least part of the year) of water in the south of the ACC to oceanic mixing and upwelling of micronutrients such as Zn. During the deglacial, vigorous upwelling led to an increase in oceanic sources of micronutrients to the surface, and an increase in surface Zn concentrations in regions downstream of a terrigenous supply (peaking at 10–15 ky BP). Error bars show 1 σ_{SE} (for age bins where $n \geq 2$). There are no data from KC081 for the age bins 0–5 ky and 25–30 ky.

3.3.2. Subantarctic Zone

[23] In contrast to the southern sites, the micronutrients at the site to the north of the modern Polar Front show a minimum during the deglacial (10–20 ky BP; Figure 5). This minimum coincides with the reduction in dust supply to the Southern Ocean, as observed in ice core records [*Delmonte et al.*, 2002], and is consistent with the greater sensitivity of the subantarctic to dust relative to areas near the Polar Front and the Antarctic islands. However, there is then an increase in micronutrient supply to the subantarctic after 10 ky BP, indicating the source of the micronutrients may be linked to the position of the westerlies in relation to the ACC, and Antarctic and subantarctic oceanic fronts in addition to changes in atmospheric input.

3.3.3. The Role of the Westerlies?

[24] The position of the westerlies may have been important in controlling oceanic upwelling processes during the deglacial [e.g., *Toggweiler et al.*, 2006]. Paleoclimate records indicate the westerlies were located to the north of their current position at the LGM and glacial termination [*Lamy et al.*, 1999; *Moreno et al.*, 1999; *Stuut and Lamy*, 2004; *Bard and Rickaby*, 2009]. The northerly position of the westerlies may have led to a greater supply of nutrients, and trace metals, to the current day subantarctic region, and greater biological productivity compared to the Holocene [*Frank et al.*, 2000; *Chase et al.*, 2003; *Dezileau et al.*, 2003]. After the LGM, the westerlies experienced a southward shift during the deglaciation [*Lamy et al.*, 1999; *Moreno et al.*, 1999; *Stuut and Lamy*, 2004; *Bard and Rickaby*, 2009]. Stronger and more southerly westerlies may also have increased the supply of nutrients [*Anderson et al.*, 2009] and micronutrients such as Zn through deeper vertical mixing with underlying waters, lateral transport of terrigenous sediments, subsurface mixing and, on a more localized scale, iceberg derived material [*Vernet et al.*, 2011]. This nutrient supply, fed from below, would have supported the temporarily enhanced biological productivity in the deglacial Southern Ocean [*Sachs and

Anderson, 2005; *Beucher et al.*, 2007; *Anderson et al.*, 2009; *Bridoux and Ingalls*, 2010].

3.3.4. The Link With Sea-Ice?

[25] The relatively early increase in micronutrient availability and diatom production, especially at the southern site PC034, is consistent with an expansion of the seasonal sea-ice zone following the coldest part of the glacial [*Jouzel et al.*, 2007]. Enhanced upwelling to the south of the modern day Polar Front, as a result of the shift in the westerlies, also brought warm waters near the surface, aiding the melting of sea-ice during the deglacial. Despite the formation of sea-ice in winter, the exposure of surface waters to wind stress in summer could have promoted some supply of micronutrients from oceanic sources and sea-ice melt [*Smith and Nelson*, 1985; *Tagliabue and Arrigo*, 2006].

[26] The geographical distribution of micronutrients from the $(Zn/Si)_{opal}$ records is consistent with significant inputs from both lateral transport and vertical upwelling and mixing in the ACC during the deglacial. Enhanced upwelling and mixing as a result of the southwards shift in the westerlies forms a plausible scenario to explain the geographical distribution of micronutrients indicated by our $(Zn/Si)_{opal}$ records. Melting of sea-ice on a seasonal basis, linked to greater upwelling and wind stress, led to further supply of micronutrients to surface waters. Regardless of the nature of the oceanic source (mixing of sediment-derived material, or upwelling of deepwaters), supply of dissolved Zn is inherently linked to the supply of other nutrients and inorganic carbon [*Archer et al.*, 2003; *Menviel et al.*, 2008; *Anderson et al.*, 2009]. While caveats exist, the implications for micronutrient supply to the Southern Ocean, biological productivity and carbon cycling of such a scenario warrants further investigation into the $(Zn/Si)_{opal}$ proxy and the collection of more data with development of well-constrained age models.

4. Summary

[27] A complex interplay of physical and biological processes control surface ocean productivity and nutrient conditions over glacial-interglacial timescales in the Southern Ocean. Micronutrient availability, one of the most important limiting factors in the modern Southern Ocean HNLC region, was relatively low during the late glacial and became enhanced during the late glacial (20–22 ky BP) and into the deglacial (15–20 ky BP) in large regions of the Atlantic sector of the Southern Ocean. With enhanced sea-ice break up in the summer months post-22 ky BP, due to peak summer insolation, diatom productivity began to increase. Consistently lower $(Zn/Si)_{opal}$ to the west of South Georgia, compared to the east, indicate the persistent direction of the westerlies and the ACC play an important role in nutrient supply, and maintains an east-west zonal asymmetry in the Atlantic sector of the ACC over glacial-interglacial timescales. During the deglacial, the increase in strong winds and vigorous upwelling allowed micronutrients such as Zn to be supplied more readily from lateral and vertical oceanic sources to a geographically widespread seasonal sea-ice zone.

Acknowledgments

[28] The authors would like to thank Claus-Dieter Hillenbrand (British Antarctic Survey) for assistance with core sampling; John Arden and David Harding for assistance in the laboratory; editor Louis Derry, an anonymous associate editor and two anonymous reviewers for constructive criticisms. This work was funded by NERC/S/A/2004/12390 and the Antarctic Funding Initiative grant AFI4–02.

References

Abelmann, A., R. Gersonde, G. Cortese, G. Kuhn, and V. Smetacek (2006), Extensive phytoplankton blooms in the Atlantic sector of the glacial Southern Ocean, *Paleoceanography*, *21*, PA1013, doi:10.1029/2005PA001199.

Allen, C. S., J. Pike, C. J. Pudsey, and A. Leventer (2005), Submillenial variations in ocean conditions during deglaciation based on diatom assemblages from the southwest Atlantic, *Paleoceanography*, *20*, PA2012, doi:10.1029/2004PA001055.

Allen, C. S., J. Pike, and C. J. Pudsey (2011), Last glacial-interglacial sea-ice cover in the SW Atlantic and its potential role in global deglaciation, *Quat. Sci. Rev.*, doi:10.1016/j.quascirev.2011.04.002.

Andersen, M. B., et al. (2011), The Zn abundance and isotopic composition of diatom frustrules, a proxy for Zn availability in ocean surface seawater, *Earth Planet. Sci. Lett.*, *301*, 137–145, doi:10.1016/j.epsl.2010.10.032.

Anderson, R. F., et al. (2009), Wind-driven upwelling in the Southern Ocean and the deglacial rise in atmospheric CO_2, *Science*, *323*, 1443–1448, doi:10.1126/science.1167441.

Archer, D. E., et al. (2003), Model sensitivity in the effect of Antarctic sea ice and stratification on atmospheric pCO_2, *Paleoceanography*, *18*(1), 1012, doi:10.1029/2002PA000760.

Ardelan, M. V., et al. (2010), Natural iron enrichment around the Antarctic Peninsula in the Southern Ocean, *Biogeosciences*, *7*, 11–25, doi:10.5194/bg-7-11-2010.

Armand, L., X. Crosta, O. Romero, and J. J. Pichon (2005), The biogeography of major diatom taxa in Southern Ocean surface sediments: 1. Sea ice related species, *Palaeogeogr. Palaeoclimatol. Palaeoecol.*, *223*, 93–126, doi:10.1016/j.palaeo.2005.02.015.

Bard, E., and R. E. M. Rickaby (2009), Migration of the subtropical front as a modulator of glacial climate, *Nature*, *460*, 380–383, doi:10.1038/nature08189.

Beucher, C. P., M. A. Brzezinski, and X. Crosta (2007), Silicic acid dynamics in the glacial sub-Antarctic: Implications for the silicic acid leakage hypothesis, *Global Biogeochem. Cycles*, *21*, GB3015, doi:10.1029/2006GB002746.

Bridoux, M. C., and A. E. Ingalls (2010), Structural identification of long-chain polyamines associated with diatom biosilica in a Southern Ocean sediment core, *Geochim. Cosmochim. Acta*, *74*, 4044–4057, doi:10.1016/j.gca.2010.04.010.

Brzezinski, M. A., J. L. Jones, and M. S. Demarest (2005), Control of silica production by iron and silicic acid during the Southern Ocean Iron Experiment (SOFeX), *Limnol. Oceanogr.*, *50*, 810–824, doi:10.4319/lo.2005.50.3.0810.

Burckle, L. H., and D. W. Cooke (1983), Late Pleistocene Eucampia antarctica abundance stratigraphy in the Atlantic sector of the Southern Ocean, *Micropaleontology*, *29*, 6–10, doi:10.2307/1485648.

Chase, Z., et al. (2003), Accumulation of biogenic and lithogenic material in the Pacific sector of the Southern Ocean during the past 40,000 years, *Deep Sea Res., Part II*, *50*, 799–832, doi:10.1016/S0967-0645(02)00595-7.

Clarke, A., M. P. Meredith, M. I. Wallace, M. A. Brandon, and D. N. Thomas (2008), Seasonal and interannual variability in temperature, chlorophyll and macronutrients in Ryder Bay, northern Marguerite Bay, Antarctica, *Deep Sea Res., Part II*, *55*, 1988–2006, doi:10.1016/j.dsr2.2008.04.035.

Crosta, X., J. J. Pichon, and L. H. Burckle (1998), Application of modern analogue technique to marine Antarctic diatoms: Reconstruction of maximum sea-ice extent a the Last Glacial Maximum, *Paleoceanography*, *13*, 284–297, doi:10.1029/98PA00339.

Dezileau, L., et al. (2003), Late Quaternary changes in biogenic opal fluxes in the Southern Indian Ocean, *Mar. Geol.*, *202*, 143–158, doi:10.1016/S0025-3227(03)00283-4.

Delmonte, B., J. R. Petit, and V. Maggi (2002), Glacial to Holocene implications of the new 27000-year dust record from the EPICA Dome C (East Antarctic) ice core, *Clim. Dyn.*, *18*, 647–660, doi:10.1007/s00382-001-0193-9.

Dixit, S., and P. Van Cappellen (2002), Surface chemistry and reactivity of biogenic silica, *Geochim. Cosmochim. Acta*, *66*, 2559–2568, doi:10.1016/S0016-7037(02)00854-2.

Dulaiova, H., M. V. Ardelan, P. Henderson, and M. A. Charette (2009), Shelf-derived iron inputs drive biological productivity in the southern Drake Passage, *Global Biogeochem. Cycles*, *23*, GB4014, doi:10.1029/2008GB003406.

Dymond, J., et al. (1992), Barium in deep-sea sediment: A geochemical indicator of paleoproductivity, *Paleoceanography*, *7*, 163–181, doi:10.1029/92PA00181.

Edwards, R., P. Sedwick, V. Morgan, and C. Boutron (2006), Iron in ice cores from Law Dome: A record of atmospheric iron deposition for maritime East Antarctica during the Holocene and Last Glacial Maximum, *Geochem. Geophys. Geosyst.*, *7*, Q12Q01, doi:10.1029/2006GC001307.

Ellwood, M. J., and K. A. Hunter (1999), Determination of the Zn/Si ratio in diatom opal: A method for the separation, cleaning and dissolution of diatoms, *Mar. Chem.*, *66*, 149–160, doi:10.1016/S0304-4203(99)00037-7.

Ellwood, M. J., and K. A. Hunter (2000a), The incorporation of zinc and iron into the frustrule of the marine diatom *Thalassiosira pseudonana*, *Limnol. Oceanogr.*, *45*, 1517–1524, doi:10.4319/lo.2000.45.7.1517.

Ellwood, M. J., and K. A. Hunter (2000b), Variations in the Zn/Si record over the last interglacial glacial transition, *Paleoceanography*, *15*, 506–514, doi:10.1029/1999PA000470.

Frank, N., et al. (2000), Similar glacial and interglacial export productivity in the Atlantic sector of the Southern Ocean: Multiproxy evidence and implications for glacial atmospheric CO_2, *Paleoceanography*, *15*, 642–658, doi:10.1029/2000PA000497.

Gersonde, R., and U. Zielinski (2000), The reconstruction of late Quaternary Antarctic sea-ice distribution—The use of diatoms as sea-ice proxies, *Palaeogeogr. Palaeoclimatol. Palaeoecol.*, *162*, 263–286, doi:10.1016/S0031-0182(00)00131-0.

Gersonde, R., et al. (2003), Last glacial sea surface temperatures and sea-ice extent in the Southern Ocean (Atlantic-Indian sector): A multiproxy approach, *Paleoceanography*, *18*(3), 1061, doi:10.1029/2002PA000809.

Gersonde, R., X. Crosta, A. Abelmann, and L. Armand (2005), Sea-surface temperature and sea ice distribution of the Southern Ocean at the EPILOG Last Glacial Maximum—A circum-Antarctic view based on siliceous microfossil records, *Quat. Sci. Rev.*, *24*, 869–896, doi:10.1016/j.quascirev.2004.07.015.

Hays, J. D., et al. (1976), Reconstruction of the Atlantic and western Indian Ocean sectors of 18 000BP Antarctic Ocean, *Mem. Geol. Soc. Am.*, *145*, 337–372.

Hendry, K. R., and R. E. M. Rickaby (2008), Opal (Zn/Si) ratios as a nearshore geochemical proxy in coastal Antarctica, *Paleoceanography*, *23*, PA2218, doi:10.1029/2007PA001576.

Hendry, K. R., M. P. Meredith, C. I. Measures, D. S. Carson, and R. E. M. Rickaby (2010), The role of sea ice formation in cycling of aluminum in northern Marguerite Bay, Antarctica, *Estuarine Coastal Shelf Sci.*, *87*, 103–112, doi:10.1016/j.ecss.2009.12.017.

Hernandez-Sanchez, M. T., et al. (2010), Productivity variation around the Crozet Plateau: A naturally iron fertilized area of the Southern Ocean, *Org. Geochem.*, *41*, 767–778, doi:10.1016/j.orggeochem.2010.05.014.

Holm-Hansen, O., M. Kahru, and C. D. Hewes (2005), Deep chlorophyll a maxima (DCMs) in pelagic Antarctic waters. II. Relation to bathymetric features and dissolved iron concentrations, *Mar. Ecol. Prog. Ser.*, *297*, 71–81, doi:10.3354/meps297071.

Jaccard, T., D. Ariztegui, and K. J. Wilkinson (2009), Incorporation of zinc into the frustrule of the freshwater diatom Stephanodiscus hantzschii, *Chem. Geol.*, *265*, 381–386, doi:10.1016/j.chemgeo.2009.04.016.

Jouzel, J., et al. (2007), Orbital and millennial Antarctic climate variability over the past 800,000 years, *Science*, *317*, 793–796, doi:10.1126/science.1141038.

Kahru, M., B. G. Mitchell, S. T. Gille, C. D. Hewes, and O. Holm-Hansen (2007), Eddies enhance biological production in the Weddell-Scotia Confluence, *Geophys. Res. Lett.*, *34*, L14603, doi:10.1029/2007GL030430.

Koning, E., et al. (2007), Rapid post-mortem incorporation of aluminum in diatom frustules: Evidence from chemical and structural analyses, *Mar. Chem.*, *106*, 208–222, doi:10.1016/j.marchem.2006.06.009.

Korb, R. E., M. J. Whitehouse, and P. Ward (2004), SeaWIFS in the southern ocean: Spatial and temporal variability in phytoplankton biomass around South Georgia, *Deep Sea Res., Part II*, *51*, 99–116, doi:10.1016/j.dsr2.2003.04.002.

Lal, D., et al. (2006), Paleo-ocean chemistry records in marine opal: Implications for fluxes of trace elements, cosmogenic nuclides (^{10}Be and ^{26}Al), and biological productivity, *Geo-*

chim. Cosmochim. Acta, *70*, 3275–3289, doi:10.1016/j.gca.2006.04.004.

Lamy, F., D. Hebbeln, and G. Wefer (1999), High-resolution marine record of climatic change in mid-latitude Chile over the last 28,000 years based on terrigenous sediment parameters, *Quat. Res.*, *51*, 83–93, doi:10.1006/qres.1998.2010.

Lefèvre, N., and A. J. Watson (1999), Modeling the geochemical cycle of iron in the oceans and it impact on atmospheric CO_2 concentrations, *Global Biogeochem. Cycles*, *13*, 727–736, doi:10.1029/1999GB900034.

Marinov, I., et al. (2008), Impact of oceanic circulation on biological carbon storage in the ocean and atmospheric pCO_2, *Global Biogeochem. Cycles*, *22*, GB3007, doi:10.1029/2007GB002958.

Martin, J. H. (1990), Glacial-Interglacial CO_2 change: The Iron Hypothesis, *Paleoceanography*, *5*, 1–13, doi:10.1029/PA005i001p00001.

Measures, C. I., and S. Vink (2001), Dissolved Fe in the upper waters of the Pacific sector of the Southern Ocean, *Deep Sea Res., Part II*, *48*, 3913–3941, doi:10.1016/S0967-0645(01)00074-1.

Menviel, L., A. Timmerman, A. Mouchet, and O. Timm (2008), Climate and marine carbon cycle response to change in the strength of Southern Hemispheric westerlies, *Paleoceanography*, *23*, PA4201, doi:10.1029/2008PA001604.

Meredith, M. P., A. C. Naveira Garabato, A. L. Gordon, and G. C. Johnson (2008), Evolution of the deep and bottom waters of the Scotia Sea, Southern Ocean, during 1995–2005, *J. Clim.*, *21*, 3327–3343, doi:10.1175/2007JCLI2238.1.

Meskhidze, N., A. Nenes, W. L. Chameides, C. Luo, and N. Mahowald (2007), Atlantic Southern Ocean productivity: Fertilization from above or below?, *Global Biogeochem. Cycles*, *21*, GB2006, doi:10.1029/2006GB002711.

Minas, H. J., and M. Minas (1992), Net community production in "high-nutrient low-chlorophyll" waters of the tropical and Antarctic oceans: Grazing versus iron hypothesis, *Oceanol. Acta*, *15*, 145–162.

Moore, K. J., M. R. Abbott, and J. G. Richman (1999), Location and dynamics of the Antarctic Polar Front from satellite sea surface temperature data, *J. Geophys. Res.*, *104*(C2), 3059–3073, doi:10.1029/1998JC900032.

Moreno, P. I., T. V. Lowell, G. L. Jacobson, and G. H. Denton (1999), Abrupt vegetation and climate changes during the Last Glacial Maximum and last termination in the Chilean Lake District: A case study from Canal De La Puntilla (41°S), *Geogr. Ann.*, *81*, 285–311, doi:10.1111/j.0435-3676.1999.00059.x.

Naveira Garabato, A. C., K. J. Heywood, and D. P. Stevens (2002), Modification and pathways of Southern Ocean deep waters in the Scotia Sea, *Deep Sea Res., Part I*, *49*, 681–705, doi:10.1016/S0967-0637(01)00071-1.

Naveira Garabato, A. C., D. P. Stevens, and K. J. Heywood (2003), Water mass conversion. fluxes, and mixing in the Scotia Sea diagnosed by an inverse model, *J. Phys. Oceanogr.*, *33*, 2565–2587, doi:10.1175/1520-0485(2003)033<2565:WMCFAM>2.0.CO;2.

Planquette, H., et al. (2007), Dissolved iron in the vicinity of the Crozet Islands, Southern Ocean, *Deep Sea Res., Part II*, *54*, 1999–2019, doi:10.1016/j.dsr2.2007.06.019.

Pugh, R. S., et al. (2009), Circum-Antarctic age modelling of Quaternary marine cores under the Antarctic Circumpolar Current: Ice-core dust-magnetic correlation, *Earth Planet. Sci. Lett.*, *284*, 113–123, doi:10.1016/j.epsl.2009.04.016.

Röthlisberger, R., M. Bigler, E. W. Wolff, F. Joos, E. Monnin, and M. A. Hutterli (2004), Ice core evidence for the extent of past atmospheric CO_2 change due to iron fertilization, *Geophys. Res. Lett.*, *31*, L16207, doi:10.1029/2004GL020338.

Sachs, J. P., and R. F. Anderson (2005), Increased productivity in the subantarctic ocean during Heinrich events, *Nature*, *434*, 1118–1121, doi:10.1038/nature03544.

Shemesh, A., R. A. Mortlock, R. J. Smith, and P. N. Froelich (1988), Determination of Ge/Si in marine siliceous microfossils: Separation, cleaning and dissolution of diatoms and radiolaria, *Mar. Chem.*, *25*, 305–323, doi:10.1016/0304-4203(88)90113-2.

Smith, W. O., and D. M. Nelson (1985), Phytoplankton bloom produced by a receding ice edge in the Ross Sea: Spatial coherence with the density field, *Science*, *227*, 163–166, doi:10.1126/science.227.4683.163.

Stuut, J.-B. W., and F. Lamy (2004), Climate variability at the southern boundaries of the Namib (southwestern Africa) and Atacama (northern Chile) coastal deserts during the last 120,000 years, *Quat. Res.*, *62*, 301–309, doi:10.1016/j.yqres.2004.08.001.

Tagliabue, A., and K. R. Arrigo (2006), Processes governing the supply of iron to phytoplankton in stratified seas, *J. Geophys. Res.*, *111*, C06019, doi:10.1029/2005JC003363.

Toggweiler, J. R., and B. Samuels (1993), Is the magnitude of the deep outflow from the Atlantic Ocean actually governed by the Southern Hemisphere winds?, in *The Global Carbon Cycle*, *NATP ASI Ser. 1*, vol. 15, edited by M. Heimann, pp. 303–331, Springer, New York.

Toggweiler, J. R., J. L. Russell, and S. R. Carson (2006), Midlatitude westerlies, atmospheric CO_2 and climate change during the ice ages, *Paleoceanography*, *21*, PA2005, doi:10.1029/2005PA001154.

Van Bennekom, A. J. (1981), On the role of aluminum in the dissolution kinetics of diatom frustules, in *6th Diatom Symposium*, edited by R. Ross, pp. 445–454, Koeltz, Koenigstein, Germany.

Van Bennekom, A. J., et al. (1989), Aluminium-rich opal: An intermediate in the preservation of biogenic silica in the Zaire (Congo) deep sea fan, *Deep Sea Res.*, *36*, 173–190, doi:10.1016/0198-0149(89)90132-5.

Vernet, M., K. Sines, D. Chakos, A. O. Cefarelli, and L. Ekern (2011), Impacts on phytoplankton dynamics by free-drifting icebergs in the NW Weddell Sea, *Deep Sea Res., Part II*, *58*, 1422–1435, doi:10.1016/j.dsr2.2010.11.022.